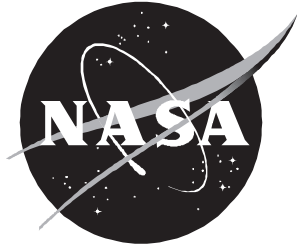


NASA/CR-1999-209547



Modeling of Longitudinal Unsteady Aerodynamics of a Wing-Tail Combination

*Vladislav Klein
The George Washington University
Joint Institute for Advancement of Flight Sciences (JIAFS)
Langley Research Center, Hampton, Virginia*

September 1999

The NASA STI Program Office . . . in Profile

Since its founding, NASA has been dedicated to the advancement of aeronautics and space science. The NASA Scientific and Technical Information (STI) Program Office plays a key part in helping NASA maintain this important role.

The NASA STI Program Office is operated by Langley Research Center, the lead center for NASA's scientific and technical information. The NASA STI Program Office provides access to the NASA STI Database, the largest collection of aeronautical and space science STI in the world. The Program Office is also NASA's institutional mechanism for disseminating the results of its research and development activities. These results are published by NASA in the NASA STI Report Series, which includes the following report types:

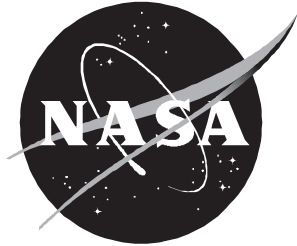
- **TECHNICAL PUBLICATION.** Reports of completed research or a major significant phase of research that present the results of NASA programs and include extensive data or theoretical analysis. Includes compilations of significant scientific and technical data and information deemed to be of continuing reference value. NASA counterpart or peer-reviewed formal professional papers, but having less stringent limitations on manuscript length and extent of graphic presentations.
- **TECHNICAL MEMORANDUM.** Scientific and technical findings that are preliminary or of specialized interest, e.g., quick release reports, working papers, and bibliographies that contain minimal annotation. Does not contain extensive analysis.
- **CONTRACTOR REPORT.** Scientific and technical findings by NASA-sponsored contractors and grantees.
- **CONFERENCE PUBLICATION.** Collected papers from scientific and technical conferences, symposia, seminars, or other meetings sponsored or co-sponsored by NASA.
- **SPECIAL PUBLICATION.** Scientific, technical, or historical information from NASA programs, projects, and missions, often concerned with subjects having substantial public interest.
- **TECHNICAL TRANSLATION.** English-language translations of foreign scientific and technical material pertinent to NASA's mission.

Specialized services that complement the STI Program Office's diverse offerings include creating custom thesauri, building customized databases, organizing and publishing research results . . . even providing videos.

For more information about the NASA STI Program Office, see the following:

- Access the NASA STI Program Home Page at <http://www.sti.nasa.gov>
- Email your question via the Internet to help@sti.nasa.gov
- Fax your question to the NASA STI Help Desk at (301) 621-0134
- Telephone the NASA STI Help Desk at (301) 621-0390
- Write to:
NASA STI Help Desk
NASA Center for AeroSpace Information
7121 Standard Drive
Hanover, MD 21076-1320

NASA/CR-1999-209547



Modeling of Longitudinal Unsteady Aerodynamics of a Wing-Tail Combination

Vladislav Klein
The George Washington University
Joint Institute for Advancement of Flight Sciences (JIAFS)
Langley Research Center, Hampton, Virginia

National Aeronautics and
Space Administration

Langley Research Center
Hampton, Virginia 23681-2199

Prepared for Langley Research Center
under Cooperative Agreement NCC1-29

September 1999

Available from:

NASA Center for AeroSpace Information (CASI)
7121 Standard Drive
Hanover, MD 21076-1320
(301) 621-0390

National Technical Information Service (NTIS)
5285 Port Royal Road
Springfield, VA 22161-2171
(703) 605-6000

Summary

Aerodynamic equations for the longitudinal motion of an aircraft with a horizontal tail were developed. In this development, emphasis was given on obtaining model structure suitable for parameter estimation from experimental data. The resulting aerodynamic models included unsteady effects in the form of linear indicial functions. These functions represented responses in the lift on the wing and tail alone, and interference between those two lifting surfaces. The effect of the wing on the tail was formulated for two different expressions concerning the downwash angle at the tail. The first expression used the Cowley-Glauert approximation known as “lag-in-downwash,” the second took into account growth of the wing circulation and delay in the development of the lift on the tail. Both approaches were demonstrated in two examples using the geometry of a fighter aircraft and a large transport. It was shown that the differences in the two downwash formulations would increase for an aircraft with long tail arm performing low-speed, rapid maneuvers.

Symbols

A_ε	amplitude ratio
a_p, a_w	lift curve slope of the tail and wing
b	wing span, m
C_a	aerodynamic force and moment coefficient
$C_{a_\alpha}(t)$ $C_{a_q}(t)$	indicial functions of the aircraft
C_L, C_m	lift and pitching-moment coefficient
$C_{Lw_{\alpha_w}}(t),$ $C_{Lw_{\alpha_t}}(t)$	indicial functions of the wing
$C_{Lt_{\alpha_w}}(t),$ $C_{Lt_{\alpha_t}}(t)$	indicial functions of the tail
$C_{Lt_g}(t)$	gust lift indicial function of the tail
$C_{m_{a.c.}}$	pitching-moment coefficient about mean aerodynamic center of the wing
c_0, c_1, \dots	parameters in indicial functions
\bar{c}	mean aerodynamic chord, m

d_{01}, d_1, \dots	spline parameters in indicial functions
$F_\varepsilon(t),$ $F_{a_\alpha}(t)$	deficiency functions
$F_{Lt_{\alpha w}}(t),$ $F_{Lt_{\alpha t}}(t)$	deficiency functions of the tail
$F_{Lw_{\alpha w}}(t)$	deficiency functions of the wing
$G_\varepsilon(ik)$	frequency response function
h	distance between <i>a.c.</i> of the wing and aircraft c.g. as a fraction of mean aerodynamic chord
$Im(\)$	imaginary part of complex number
i	imaginary unit, $i = \sqrt{-1}$
k	reduced frequency, $k = \omega \ell / V$
L	a) distance from bound vortex to reference point, m b) lift, N
ℓ	distance from wing trailing edge to tail leading edge, m
ℓ_t	tail arm, m
q	rate of pitch, sec^{-1}
$Re(\)$	real part of complex number
S	wing area, m^2
t	time, sec
V	airspeed, m/sec
V_t	tail volume, $V_t = S_t \ell_t / S \bar{c}$
w_i	induced vertical velocity, m/sec

x distance from reference point to starting vortex, m

α angle of attack

Γ circulation, m²/sec

Δ increment

δ time delay between harmonic responses, sec

ε downwash angle, rad

$\varepsilon_{CL}(t), \varepsilon_{\alpha}(t)$ downwash indicial functions

Λ aspect ratio, $\Lambda = b^2/S$

λ_j exponents in indicial functions, sec⁻¹

ρ air density, kg/m³

τ time delay, sec

φ_{ε} phase angle, rad

ω angular frequency, sec⁻¹

Superscript:

• time derivative

~ Fourier transform

' nondimensional quantity

* “lag-in-downwash” formulation

Subscript:

t tail

w wing

Derivatives of aerodynamic coefficients C_a , where index $a = L$ or m

$$C_{a_q}(\infty) \equiv C_{a_q} = \frac{\partial C_a}{\partial \frac{q\bar{c}}{2V}}, \quad C_{a_\alpha}(\infty) \equiv C_{a_\alpha} = \frac{\partial C_a}{\partial \alpha}$$

Introduction

Recently there has been an increased interest in identification of aircraft aerodynamic models that include unsteady aerodynamic terms. The majority of identified models were related to the longitudinal motion of tailless aircraft, see reference 1 to 3, where the aerodynamic models had relatively simple form. In formulating aerodynamic model equations for a wing-tail combination, however, more complicated model forms can be expected. This problem was first addressed in the early twenties by Cowley and Glauert (ref. 4). They realized that there was a time lag before the wing disturbance reaches the tail. They assumed that the downwash associated with a change in lift is equal to the corresponding steady value but the effect at the tail is delayed by the time for the airplane to travel a distance equal to the tail arm. The change of the lift on the tail due to downwash was included in the damping-in-pitch derivative. Now this change is interpreted as a tail contribution to the acceleration derivatives, i.e., the derivative of the lift and pitching moment with respect to rate of change in the angle of attack.

The investigation of the downwash angle was extended by R. T. Jones and Fehlnner in reference 5 by considering both the growth of wing circulation and the delay in the development of lift by the tail. They presented an expression for the downwash indicial function associated with a change of the lift on the wing. Considerable effort to the rigorous explanation of the downwash both qualitatively and analytically was given by Tobak in reference 6. He developed indicial functions for the lift and pitching moment of a wing-tail combination and presented numerical results for several representative cases in supersonic flight regimes. The theoretical results were then applied to the longitudinal stability analysis of an aircraft.

In reference 7 a theoretical analysis of the downwash due to changes in the lift of the wing was presented. In this analysis the wing was approximated either by a single horseshoe vortex or by a set of these vortices. The result showed that for specific changes in the lift the downwash would depend on the tail arm, wing aspect ratio and its span. Similar to reference 7, a simple vortex system was used in reference 8 to model unsteady aerodynamic effects into the longitudinal equations of motion. It was found that the solution of resulting integro-differential equations led to lengthy computations. The calculations also showed that the unsteady aerodynamics could be adequately accounted for when the unsteady effects were included only in the downwash development. This finding permitted reformulating the equations so that they appeared suitable for parameter estimation using flight test data.

This report is an extension of previous research in references 5, 7, and 8. Its purpose is to develop aerodynamic equations for the longitudinal motion of an aircraft with horizontal tail. These equations include unsteady effects modeled by linear indicial functions. The emphasis is given to obtaining model structure suitable for model identification using experimental data. It means that the postulated model should explain the aerodynamics of wing-tail combination with sufficient accuracy and, at the same time, should be simple enough to provide good conditions for parameter identifiability. The report starts with the formulation of equations for the lift and pitching-moment coefficient and introduction of indicial functions in these equations. Then the development of an indicial function relating the change in the lift of a wing due to downwash is presented. The downwash angle during the harmonic motion of an aircraft is compared with that based on the traditional “lag-in-downwash” factor contained in the acceleration stability derivatives. The variation of the downwash angle with the geometry and frequency of the harmonic motion is also briefly discussed. Next, the final form of aerodynamic model equations is pre-

sented. Numerical examples using the geometry of a fighter and transport aircraft demonstrate possible forms of indicial functions using both the “lag-in-downwash” formulation and that with unsteady terms. The report is completed by concluding remarks.

Indicial Functions

In the following development the lift and pitching moment will be considered as functions of the angle of attack and pitching velocity, i.e.,

$$C_a = C_a(\alpha, q), \quad a = L \text{ or } m$$

Then the aerodynamic model equations can be formulated as

$$C_a(t) = C_a(0) + \int_0^t C_{a_\alpha}(t-\tau) \dot{\alpha}(\tau) d\tau + \frac{\bar{c}}{2V} \int_0^t C_{a_q}(t-\tau) \dot{q}(\tau) d\tau \quad (1)$$

Where $C_a(0)$ is the value of the coefficient at initial steady-state conditions, and $C_{a_\alpha}(t)$ and $C_{a_q}(t)$ are the indicial functions defining the responses in C_a to unit step in α and q respectively. Replacing the second indicial function in (1) by its steady value $C_{a_q}(\infty)$, equation (1) is simplified as

$$C_a(t) = C_a(0) + \frac{\bar{c}}{2V} C_{a_q}(\infty) q(t) + \int_0^t C_{a_\alpha}(t-\tau) \dot{\alpha}(\tau) d\tau \quad (2)$$

When the deficiency functions

$$F_{a_\alpha}(t) = C_{a_\alpha}(\infty) - C_{a_\alpha}(t) \quad (3)$$

are substituted into (2) the equations for the aerodynamic coefficients take the form

$$C_a(t) = C_a(0) + C_{a_\alpha}(\infty) \alpha(t) + \frac{\bar{c}}{2V} C_{a_q}(\infty) q(t) - \int_0^t F_{a_\alpha}(t-\tau) \dot{\alpha}(\tau) d\tau \quad (4)$$

where $C_{a_\alpha}(\infty)$ and $C_{a_q}(\infty)$ are the rates of change with α and q of the coefficients C_L and C_m .

The indicial functions $C_{a_\alpha}(t)$ include combined responses of the wing and tail, and interference effects between those two lifting surfaces. Because of linear aerodynamics the resulting indicial functions are given as a sum of their components. For the indicial function $C_{L_\alpha}(t)$ these components will be as follows:

- (1) the response in the lift of the wing to a unit step in angle of attack of the wing, while the angle of attack of the tail remains at zero;
- (2) the response in the lift of the tail to a unit step in angle of attack of the tail, while the angle of attack of the wing remains at zero;

- (3) the response in the lift of the tail to a unit step in the angle of attack of the wing, while the angle of attack of the tail remains at zero;
- (4) the responses in the lift of the wing to a unit step in the angle of attack of the tail, while the angle of attack of the wing remains at zero.

The first two components are represented by the response of an isolated wing and isolated tail respectively. As pointed out in reference 6, these representations are true for supersonic speeds. For subsonic speeds, however, these are good approximations. The third component expresses the lift on the tail due to a change in the downwash induced by the lift of the wing. It is usually a significant contribution to the resulting pitching moment of an aircraft. Finally, the last component is zero for supersonic speeds. For subsonic speeds it can be neglected. A summary of all four components, their conditions and interpretations is given in table 1.

The expressions for the indicial function $C_{Lw_{\alpha w}}(t)$ of a wing alone were given by several authors. In reference 5, the indicial function was formed as a sum of exponential

$$C_{Lw_{\alpha w}}(t) = c_0 + \sum_j c_j e^{\lambda_j t} \quad (5)$$

where the values of parameters c_0 , c_j and λ_j depend on the wing geometry. For a wing with small aspect ratio equation (5) was further simplified as

$$C_{Lw_{\alpha w}}(t) = c_0 + c_1 e^{\lambda_1 t} \quad (6)$$

Equation (6) was used in references 1 and 3 for aerodynamic model identification of tailless aircraft from wind tunnel, small amplitude oscillatory data. In reference 2, the parameters in (6) were considered as functions of the angle of attack for the identification of nonlinear models from wind tunnel dynamic data with large amplitudes. In both cases, identified models were found to be adequate representations of experimental data.

A simple form of the indicial function $C_{Lt_{\alpha w}}(t)$ defining the downwash effect on this tail can be obtained by considering that a sudden change in the angle of attack of the wing results in a sudden change in the downwash. Downwash from the wing is delayed from reaching the tail by the time

$$\Delta t = \frac{\ell_t}{V}$$

where ℓ_t is the distance from the *a.c.* of the wing to that of the tail and V is the airspeed that remains constant and equal to the speed of undisturbed flow. By neglecting the unsteady aerodynamic effect on the tail, the indicial function $C_{Lt_{\alpha w}}(t)$ can be expressed as

$$C_{Lt_{\alpha w}}(t) = C_{Lt_{\alpha w}}(\infty)(t - \Delta t) \quad (7)$$

Its time history is sketched in figure 1a. This assumption about the downwash has been used by Cowley and Glauert in formulating contributions of the tail to the acceleration stability derivatives $C_{L_{\alpha}}$ and $C_{m_{\alpha}}$.

A more detailed qualitative assessment of $C_{Lt_{\alpha w}}(t)$ is given in reference 6. At the time of sudden change in α_w and under condition $\alpha_t = 0$, no disturbances are present at the tail. At certain time $t_1 > 0$, the tail begins to penetrate the wake created by the vorticity shed by the wing. The tail begins to

develop positive lift on that portion of its surface that has penetrated the wake. As time increases the tail further penetrates the field of shed vorticity and is subjected to a combined effect of upwash and downwash. Further penetration into the wake results in a change of lift from positive to negative. At certain time $t_2 > t_1$ the tail is fully immersed in the steady downwash field. Then the lift on the tail remains constant because it is no longer influenced by the disturbances created by the wing at the beginning of the motion.

From the preceding discussion one can anticipate the shape of $C_{L_{t_{\alpha w}}}(t)$ as sketched in figure 1b and its analytical form as a combination of three effects:

- a) change in the lift of the wing followed by a change in angle of attack of the wing;
- b) change in the downwash at the tail following a change in lift on the wing;
- c) change in the lift on the tail due to a change in downwash at the tail.

Therefore, the variation in the lift on the tail following a change in angle of attack of the wing, while maintaining $\alpha_t = 0$, follows as a solution of three equations

$$C_{L_w}(t) = C_{L_{w_{\alpha w}}}(t)\alpha(0) + \int_0^t C_{L_{w_{\alpha w}}}(t-\tau)\dot{\alpha}(\tau)d\tau \quad (8)$$

$$\varepsilon(t) = \varepsilon_{CL}(t)C_{L_w}(0) + \int_0^t \varepsilon_{CL}(t-\tau)\dot{C}_{L_w}(\tau)d\tau \quad (9)$$

$$C_{L_t}(t) = -C_{L_{t_g}}(t)\varepsilon(0) - \int_0^t C_{L_{t_g}}(t-\tau)\dot{\varepsilon}(\tau)d\tau \quad (10)$$

The minus signs in equation (10) reflect the definition of a positive downwash angle that results in a decrease of the angle of attack at the tail. The corresponding indicial function $C_{L_{t_{\alpha w}}}(t)$ can be obtained from equations (8) to (10) as

$$\varepsilon_{\alpha}(t) = \varepsilon_{CL}(t)C_{L_{w_{\alpha w}}}(0) + \int_0^t \varepsilon_{CL}(t-\tau)\dot{C}_{L_{w_{\alpha w}}}(\tau)d\tau \quad (11)$$

$$C_{L_{t_{\alpha w}}}(t) = -C_{L_{t_g}}(t)\varepsilon_{\alpha}(0) - \int_0^t C_{L_{t_g}}(t-\tau)\dot{\varepsilon}_{\alpha}(\tau)d\tau \quad (12)$$

where the last equation can be also written as

$$C_{L_{t_{\alpha w}}}(t) = -\varepsilon_{\alpha}(t)C_{L_{t_g}}(0) - \int_0^t \varepsilon_{\alpha}(t-\tau)\dot{C}_{L_{t_g}}(\tau)d\tau \quad (13)$$

In the above equation the indicial function $C_{L_{t_{\alpha w}}}(t)$ has already been discussed. The function $C_{L_{t_g}}(t)$ represents the lift on the tail during passage of the tail through a step change in downwash that is equivalent to the passage through a sharp-edge gust. The two-dimensional theory for this case was developed by Küssner in reference 9 and extended to the three-dimensional case in reference 10. It was found that the indicial function $C_{L_{t_g}}(t)$ can again be approximated by a sum of exponentials similar to equation (5) for $C_{L_{t_{\alpha w}}}(t)$.

Analytical expressions for the indicial function $\varepsilon_{CL}(t)$ in equations (9) and (11) were developed by several authors, see e.g., references 5, 7, and 8 using various degree of approximation to the vortex sheet behind the wing. A rather simple approach to this problem is demonstrated in the next section. Once the indicial function explaining the variation in lift of an aircraft following changes in the angle of attack are known, they can be converted to those in the pitching-moment equation.

Downwash Angle

In the following development the vortex sheet of a finite wing in an incompressible steady flow is replaced by a horseshoe vortex consisting of the bound vortex and two trailing vortices. After a sudden change in the circulation around wing, a stationary vortex separates from the trailing edge of the wing and moves in the direction of the velocity vector with the velocity equal to that of free stream, see figure 2. The vortex system shown in figure 3 indicates the position of a reference point A and distance between trailing vortices. For the present study this distance is equal to the wing span. As pointed out in reference 11, however, the distance between trailing vortices is less than the wing span. It can be determined by equating the lift of the replacement system to the lift of the wing.

The downwash angle at the point A is $\varepsilon = w_i/V$ where w_i is the sum of induced velocities by all four vortices. These velocities are calculated in the plane of the vortex system, midway between the two trailing vortices, from the Biot-Savart rule. The expression for the downwash angle takes the form

$$\varepsilon(x) = \frac{\Delta\Gamma}{2\pi V} \left[\frac{\frac{x}{b/2} + \frac{b/2}{x}}{\sqrt{\left(\frac{b}{2}\right)^2 + x^2}} + \frac{\frac{L}{b/2} + \frac{b/2}{L}}{\sqrt{\left(\frac{b}{2}\right)^2 + L^2}} \right] \quad (14)$$

where $\Delta\Gamma$ is the circulation strength of each four vortices and $L = 3/4\bar{c} + \ell$. It is convenient to express the downwash angle in nondimensional form as a function of time. This can be achieved by considering the relation

$$x = Vt - \ell \quad (15)$$

where ℓ is the distance between the wing trailing edge (the origin of the wing circulation) and the leading edge of the tail. By introducing nondimensional time

$$t' = \frac{V}{\ell} t \quad (16)$$

and nondimensional lengths in terms of the half span, i.e.,

$$x' = \frac{x}{b/2}, \ell' = \frac{\ell}{b/2} \text{ and } L' = \frac{L}{b/2}$$

equation (15) takes the nondimensional form

$$x' = \ell'(t' - 1) \quad (17)$$

Substituting (17) into (14) and replacing L by L' yields

$$\varepsilon(t') = \frac{\Delta\Gamma}{\pi V b} \left[\frac{\ell'(t' - 1) + \frac{1}{\ell'(t' - 1)}}{\sqrt{1 + \ell'^2(t' - 1)^2}} + \frac{L' + \frac{1}{L'}}{\sqrt{1 + L'^2}} \right] \quad (18)$$

It is further assumed that the Zhukovski's formula

$$\rho V \Delta\Gamma b = \frac{1}{2} \rho V^2 S \Delta C_L$$

can be also applied to the unsteady flow around the wing. This leads to an increment in the circulation

$$\Delta\Gamma = \frac{SV}{2b\Lambda} \Delta C_L \quad (19)$$

where $\Lambda = b^2/S$ is the wing aspect ratio. Combining (18) and (19) gives the expression for the downwash indicial function

$$\varepsilon_{CL}(t') = \frac{1}{2\pi\Lambda} \left[\frac{\ell'(t' - 1) + \frac{1}{\ell'(t' - 1)}}{\sqrt{1 + \ell'^2(t' - 1)^2}} + \frac{L' + \frac{1}{L'}}{\sqrt{1 + L'^2}} \right] \quad (20)$$

and it's steady value

$$\varepsilon_{CL}(\infty) = \frac{1}{2\pi\Lambda} \left[1 + \frac{L' + \frac{1}{L'}}{\sqrt{1 + L'^2}} \right] \quad (21)$$

The indicial function $\varepsilon_{CL}(t')$ is sketched in figure 4. It shows infinite values for $t' = 1$ which is the time when the leading edge of the tail reaches the position of the starting vortex. After that, the downwash angle decreases and, with increasing time, approaches a steady value. Although the indicial function can reach an infinite value, the convolution with the lift results in finite downwash at all points. If the wing wake passes either above or below the tail surface, the indicial function $\varepsilon_{CL}(t')$ will not have infinite values. Using the Cowley-Glauert explanation of the downwash delay and considering $L = \ell'$, the expression for the downwash indicial function is simplified as

$$\varepsilon_{CL}^*(t) = \varepsilon_{CL}(\infty) \mathbf{1}\left(t - \frac{L}{V}\right) \quad (22)$$

or

$$\varepsilon_{CL}^*(t') = \varepsilon_{CL}(\infty) \mathbf{1}\left(t' - \frac{L}{\ell}\right) \quad (23)$$

where $\mathbf{1}\left(t - \frac{L}{V}\right)$ and $\mathbf{1}\left(t' - \frac{L}{\ell}\right)$ are the unit step functions. The time history of $\varepsilon_{CL}^*(t')$ is included in figure 4 as a dashed line.

A difference in calculated downwash using indicial function given by equation (20) or (23), and the effect of geometry and flight condition will be demonstrated on the harmonic motion of an aircraft. Equation (9) has its frequency domain equivalent

$$\tilde{\varepsilon}(ik) = ik \tilde{\varepsilon}_{CL}(ik) \tilde{C}_{LW}(ik) \quad (24)$$

which leads to the frequency response function

$$G_{\varepsilon}(ik) \equiv \frac{\tilde{\varepsilon}(ik)}{\tilde{C}_{LW}(ik)} = ik \tilde{\varepsilon}_{CL}(ik) \quad (25)$$

where $k = \omega \ell / V$ is the reduced frequency and

$$\tilde{\varepsilon}_{CL}(ik) = \int_0^{\infty} \varepsilon_{CL}(t') e^{-ikt'} dt' \quad (26)$$

For the numerical evaluation of the Fourier integral in (26) it is advantageous to express the indicial function $\varepsilon_{CL}(t')$ in the form

$$\varepsilon_{CL}(t') = \varepsilon_{CL}(\infty) - F_{\varepsilon}(t')$$

where the deficiency function follows from (20) and (21) as

$$F_{\varepsilon}(t') = \frac{1}{2\pi\Lambda} \left[1 - \frac{\ell'(t'-1) + \frac{1}{\ell'(t'-1)}}{\sqrt{1 + \ell'^2(t'-1)^2}} \right] \quad (27)$$

Using equations (25) and (27) the frequency response functions relating the downwash and the lift takes the form

$$G_{\varepsilon}(ik) = \varepsilon_{CL}(\infty) - ik \int_0^{\infty} F_{\varepsilon}(t') e^{-ikt'} dt' \quad (28)$$

The computed frequency response curve $2\pi\Lambda G_{\varepsilon}(ik)$ for $\ell' = 1.0$ and $L' = 1.2$ is plotted in figure 5 as a vector diagram. In the same figure the frequency response curve based on the Cowley-Glauert's "lag-in-downwash" formulation

$$G_{\varepsilon}^*(ik) = \varepsilon_{CL}(\infty) e^{-ikL/\ell} \quad (29)$$

is also given. For the presentation of differences in both downwash formulations and their variation with the frequency and distance ℓ' , the transfer functions $G_\varepsilon(ik)$ and $G_\varepsilon^*(ik)$ defined by the previous two equations are expressed in terms of amplitudes and phase angles as

$$G_\varepsilon(ik) = A_\varepsilon e^{i\varphi_\varepsilon} \quad (30)$$

$$G_\varepsilon^*(ik) = A_\varepsilon^* e^{i\varphi_\varepsilon^*} \quad (31)$$

Then the amplitude ratio $A_\varepsilon/A_\varepsilon^*$ for three different values of $\ell' = 1.0, 0.5$ and 0.25 are plotted in figure 6. Figure 7 shows the time delay between harmonic responses obtained from equations (28) and (29) as

$$\delta' = \frac{\varphi_\varepsilon}{k} - \frac{L}{\ell} \quad (32)$$

Considering the results in figures 5 to 7, the differences in both downwash formulations depend mainly on two parameters, the reduced frequency, k , and nondimensional distance ℓ' . The effect of nondimensional tail arm $L' = \ell'_t$ is rather small as follows from equations (20) and (21). The differences in amplitude ratios increase with increased reduced frequency. Increased reduced frequency corresponds with rapid maneuvers at low airspeed for an aircraft with long tail arm. On the other hand, these differences at given reduced frequency decrease with increased parameter ℓ' . As to the differences in the time delays, an increase in reduced frequency makes these differences, in general, smaller. At a given reduced frequency the differences in time delays will decrease with the parameter ℓ' which is especially apparent at low values of k , see figure 7. More detailed assessment of both downwash formulations can be made only for specific aircraft geometry and flight conditions.

Lift and Pitching Moment

Returning to equation (4) the lift and pitching-moment coefficient are expressed as

$$C_L(t) = C_L(0) + C_{L_\alpha}(\infty)\alpha(t) + \frac{\bar{c}}{2V}C_{L_q}q(t) - \int_0^t F_{L_\alpha}(t-\tau)\dot{\alpha}(\tau)d\tau \quad (33)$$

$$C_m(t) = C_m(0) + C_{m_\alpha}(\infty)\alpha(t) + \frac{\bar{c}}{2V}C_{m_q}q(t) - \int_0^t F_{m_\alpha}(t-\tau)\dot{\alpha}(\tau)d\tau \quad (34)$$

Contributions of the wing and tail to these coefficients can be found from the relations

$$C_L(t) = C_{L_w}(t) - \frac{S_t}{S}C_{L_t}(t) \quad (35)$$

$$C_m(t) = C_{m_{a.c.}} + hC_L(t) - V_t C_{L_t}(t) \quad (36)$$

where $C_{m_{a.c.}}$ is the pitching moment about the aerodynamic center of the wing, *a.c.*, h is the distance between the *a.c.* and the aircraft center of gravity expressed as a fraction of \bar{c} , $V_t = S_t \ell'_t / S \bar{c}$ is the tail volume and C_{L_t} is based on S_t .

Combing equations (33) through (36) yields

$$C_L(t) = C_L(0) + C_{L_\alpha}(\infty)\alpha(t) + \frac{\bar{c}}{2V}C_{L_q}(\infty)q(t) - \int_0^t \left[F_{L_{w_{\alpha w}}}(t-\tau) + \frac{S_t}{S}F_{L_{t_{\alpha t}}}(t-\tau) + \frac{S_t}{S}F_{L_{t_{\alpha w}}}(t-\tau) \right] \dot{\alpha}(\tau) d\tau \quad (37)$$

$$C_m(t) = C_m(0) + C_{m_\alpha}(\infty)\alpha(t) + \frac{\bar{c}}{2V}C_{m_\alpha}(\infty)q(t) - \int_0^t [hF_{L_{w_{\alpha w}}}(t-\tau) - V_t F_{L_{t_{\alpha t}}}(t-\tau) - V_t F_{L_{t_{\alpha w}}}(t-\tau)] \dot{\alpha}(\tau) d\tau \quad (38)$$

where the deficiency functions are defined as

$$F_{L_{w_{\alpha w}}}(t) = C_{L_{w_{\alpha w}}}(\infty) - C_{L_{w_{\alpha w}}}(t) \quad (39)$$

$$F_{L_{t_{\alpha t}}}(t) = C_{L_{t_{\alpha t}}}(\infty) - C_{L_{t_{\alpha t}}}(t) \quad (40)$$

$$F_{L_{t_{\alpha w}}}(t) = C_{L_{t_{\alpha w}}}(\infty) - C_{L_{t_{\alpha w}}}(t) \quad (41)$$

As mentioned earlier, the steady parts of indicial functions in equations (37) and (38) are aircraft stability derivatives C_{L_α} , C_{m_α} , C_{L_q} and C_{m_q} . The first two are usually formed as

$$C_{L_\alpha} = a_w \left[1 + \frac{a_t}{a_w} \frac{S_t}{S} \left(1 - \frac{\partial \epsilon}{\partial \alpha} \right) \right] \quad (42)$$

$$C_{m_\alpha} = a_w \left[h - \frac{a_t}{a_w} V_t \left(1 - \frac{\partial \epsilon}{\partial \alpha} \right) \right] \quad (43)$$

where the contributions of the wing and tail are easily recognized. In these expressions $a_w = C_{L_{w_{\alpha w}}}(\infty)$ and $a_t = C_{L_{t_{\alpha t}}}(\infty)$ are the lift curve slopes of the wing and tail respectively.

The derivatives C_{L_q} and C_{m_q} represent aerodynamic effects that accompany rotation of the aircraft about its lateral axis while α remains constant. Both the wing and tail are affected by the rotation but the wing contribution is usually negligible. A discussion of the damping term C_{m_q} due to wing in supersonic flight conditions is contained in reference 6. The contribution of the tail includes changes in the lift on the tail due to increased angle of attack by $(q\ell_t)/V$ and changes due to effective angle of attack at the tail caused by the pitching velocity of the wing. The latter change in the lift is discussed in references 12 and 13 for supersonic flight regimes. Thus considering a contribution of the tail only, the damping derivatives are approximated as

$$C_{L_q} \approx 2a_t V_t \quad (44)$$

$$C_{m_q} \approx -2a_t \frac{\ell}{\bar{c}} V_t \quad (45)$$

Examples

In the following examples, the indicial functions $C_{L_\alpha}(t)$ and $C_{m_\alpha}(t)$ were computed using two sets of data representing a fighter and transport aircraft. The geometrical characteristics of these aircraft are summarized in table 2. The approximate expressions for the indicial functions of the wing and tail, $C_{L_{w_{\alpha w}}}(t)$ and $C_{L_{t_{\alpha t}}}(t)$, and the gust lift function $C_{L_t}(t)$ were taken from reference 14. The functions for given aspect ratios and argument $t' = V_t/\ell$ have the form

for fighter aircraft:

$$\begin{aligned} C_{L_{w_{\alpha w}}}(t') &= 3.77(1 - 0.283e^{-0.626t'}) \\ C_{L_{t_{\alpha t}}}(t') &= 4.65(1 - 0.361e^{-0.442t'}) \\ C_{L_t}(t') &= 4.65(1 - 0.448e^{-0.336t'} - 0.272e^{-0.841t'} - 0.193e^{-3.48t'}) \end{aligned}$$

for transport aircraft:

$$\begin{aligned} C_{L_{w_{\alpha w}}}(t') &= 4.65(1 - 0.361e^{-3.12t'}) \\ C_{L_{t_{\alpha t}}}(t') &= 3.77(1 - 0.283e^{-2.20t'}) \\ C_{L_t}(t') &= 3.77(1 - 0.679e^{-3.23t'} - 0.227e^{-18.5t'}) \end{aligned}$$

The indicial functions $\varepsilon_{CL}(t')$ and $\varepsilon_{CL}^*(t')$ were computed from equations (20) and (23), indicial function $C_{L_{t_{\alpha w}}}(t')$ from equations (11) and (13). The resulting indicial functions $C_{L_\alpha}(t')$ and $C_{m_\alpha}(t')$ were obtained from equations (35) and (36) as

$$C_{L_\alpha}(t') = C_{L_{w_{\alpha w}}}(t') + \frac{S_t}{S}(C_{L_{t_{\alpha t}}}(t') + C_{L_{t_{\alpha w}}}(t')) \quad (46)$$

$$C_{m_\alpha}(t') = hC_{L_\alpha}(t') - V_T(C_{L_{t_{\alpha t}}}(t') + C_{L_{t_{\alpha w}}}(t')) \quad (47)$$

assuming $C_{m_{a.c.}} = 0$.

The three indicial functions of the fighter aircraft appearing on the right side of equations (46) and (47) are plotted in figure 8, the functions $C_{L_\alpha}(t')$ and $C_{m_\alpha}(t')$ in figure 9. The dashed lines in these figures indicate the “lag-in-downwash” approximation of the indicial function $\varepsilon_{CL}(t')$. Figure 10 and 11 present the same functions as above for the transport aircraft. As expected, the form of the indicial functions $C_{L_\alpha}(t')$ for both aircraft was only slightly affected by different expressions for $\varepsilon_{CL}(t')$. This means that the model structure for $C_{L_\alpha}(t')$ can be postulated as that for the wing alone, i.e.,

$$C_{L_\alpha}(t) = c_o + \sum_j c_j e^{\lambda_j t}$$

The structure for an adequate model for $C_{m_\alpha}(t')$, on the other hand, could be strongly affected by $\varepsilon_{CL}(t')$, evaluated either from equation (20) or (23). As mentioned previously, the decision between using one of the forms for $\varepsilon_{CL}(t')$ will depend on the values of two parameters, k and ℓ' . Assuming a harmonic motion with $\omega = 4$ rad/sec and $V = 100$ m/sec, and given geometry, then for the fighter aircraft $k = 0.08$ and $\ell' = 0.44$. Using figures 6 and 7 it can be found that the amplitude ratio, $A_\varepsilon \approx 1.0$ and time delay $\delta \approx 0.017$ sec. In this case, therefore, the Cowley-Glauert approximation for $\varepsilon_{CL}(t')$ would be warranted. For the transport aircraft $k = 0.96$ and $\ell' = 0.80$ which resulted in $A_\varepsilon \approx 2.0$ and $\delta \approx 0.12$ sec. In this case, equation (20) for $\varepsilon_{CL}(t')$ should be used. Then the model for $C_{m_\alpha}(t')$ can be postulated as

$$C_{m_\alpha}(t) = d_0 + d_1(t-t_1)_+^0 \quad (49)$$

or

$$C_{m_\alpha}(t) = d_0 + d_1 t + d_2(t-t_1)_+ + d_3(t-t_2)_+ \quad (50)$$

The plus functions in (49) and (50) are defined as

$$(t-t_1)_+^0 = \begin{cases} 1 & \text{for } t_1 \geq t \\ 0 & \text{for } t_1 < t \end{cases}$$

$$(t-t_1)_+ = \begin{cases} t-t_1 & \text{for } t_1 \geq t \\ 0 & \text{for } t_1 < t \end{cases}$$

and similiary for $(t-t_2)_+$.

Equation (49) reflects sudden change in the downwash angle, whereas equation (50) takes into account gradual changes in the downwash. In equation (49) the value of d_0 would be different from that based on Cowley-Glauert's approximation of $\varepsilon_{CL}(t)$. The time t_1 in both expressions might be close to $t = \ell_t/V$.

Concluding Remarks

Aerodynamic model equations for the longitudinal motion of an aircraft with horizontal tail were developed. The equations include unsteady effects modeled by linear indicial functions. These functions represent responses in the lift and tail alone, and interference between those two lifting surfaces. The indicial functions for the lift on the wing and tail were modeled by a series of exponential functions. The effect of the wing on the tail was formulated for two different expressions for the downwash angle at the tail. The first expression used the Cowley-Glauert approximation known as "lag-in-downwash." The second took into account growth of the wing circulation and delay in the development of the lift by the tail. From analytical expressions obtained and numerical examples, the following conclusions can be drawn:

- a) for harmonic motion the differences in calculated downwash using simple "lag-in-downwash" concept and that with unsteady aerodynamics depend upon the frequency and airspeed of the motion, on the distance between the wing trailing edge and tail leading edge, and on the wing

span. These differences will increase for an aircraft with long tail arm performing rapid maneuvers at low speed. More detailed assessment of both concepts, however, can be made for specified aircraft geometry and flight conditions;

- b) a model for the lift is only slightly affected by different approaches in computing the downwash angle. For the preliminary studies and model identification, the model structure can be the same as that for the wing alone;
- c) in pitching-moment formulation the “lag-in-downwash” approximation is warranted for aircraft with short tail arms. For aircraft with long tail arms, however, the expression with unsteady terms should be considered. Then the resulting indicial function for the pitching moment can be approximated by zero-order or first-order splines.

References

1. Klein, Vladislav; Murphy, Patrick C.; Curry, Timothy J.; and Brandon, Jay M.: *Analysis of Wind Tunnel Longitudinal Static and Oscillatory Data of the F-16XL Aircraft*. NASA/TM-97-20676, 1997.
2. Klein, Vladislav; and Murphy, Patrick C.: *Estimation of Aircraft Nonlinear Unsteady Parameters From Wind Tunnel Data*. NASA/TM-1998-208969, 1998.
3. Smith, Mark S.: *Analysis of Wind Tunnel Oscillatory Data of the X-31A Aircraft*. M.S. Thesis, The George Washington University, Washington, D.C., 1998.
4. Cowley, W. L.; and Glauert H.: *The Effect of the Lag of the Downwash on the Longitudinal Stability of an Airplane and on the Rotary Derivative M_q* . R. & M. 718, Feb. 1921.
5. Jones, Robert T.; and Fehlner, Leo F.: *Transient Effects of the Wing Wake on the Horizontal Tail*. NACA TN-771, 1940.
6. Tobak, Murray: *On the Use of Indicial Function Concept in the Analysis of Unsteady Motions of Wings and Wing-Tail Combinations*. NACA Rep. 1188, 1954.
7. Danek, M.: *Downwash Angle at the Horizontal Tail During Rapid Oscillations of an Aircraft*. Internal Report, Military-Technical Academy (VTA), Brno, Czech Republic, 1956.
8. Queijo, M. J.; Wells, William R. and Keskar, Dinesh A.: *Inclusion of Unsteady Aerodynamics in Longitudinal Parameter Estimation From Flight Data*. NASA TP-1536, 1979.
9. Küssner, H. G.: *Zusammenfassender Bericht über den instationären Auftrieb von Flügeln*. *Luftfahrtforschung*, Bd. 13, Nr. 12, Dec. 1936, pp. 410–424.
10. Jones, Robert T.: *The Unsteady Lift of a Wing of Finite Aspect Ratio*. NACA TR No. 681, 1940.
11. Krasnov, N. F.: *Aerodynamics*. NASA TT F-765, 1978, pp. 234–239.
12. Ribner, Herbert S.: *Time-Dependent Downwash at the Tail and Pitching Moment Due to Normal Acceleration at Supersonic Speeds*. NACA TN-2042, 1950.
13. Martin, John C.; Diederich, Margaret S.; and Bobbitt, Percy J.: *A Theoretical Investigation of the Aerodynamics of Wing-Tail Combinations Performing Time-Dependent Motions at Supersonic Speeds*. NACA TN-3072, 1954.
14. Jones, Robert T.: *The Unsteady Lift of a Wing of Finite Aspect Ratio*. NACA Rep. 681, 1939.

Table 1. Summary of components of indicial functions expressing changes in lift due to unit step in angle of attack.

Component	Indicial Function	Conditions	Interpretation
1	$C_{Lw_{\alpha_w}}(t)$	$\alpha_w = \mathbf{1}(t), \alpha_t = 0$	lift response of isolated wing
2	$C_{Lt_{\alpha_t}}(t)$	$\alpha_w = 0, \alpha_t = \mathbf{1}(t)$	lift response of isolated tail
3	$C_{Lt_{\alpha_w}}(t)$	$\alpha_w = \mathbf{1}(t), \alpha_t = 0$	lift due to downwash
4	$C_{Lw_{\alpha_t}}(t)$	$\alpha_w = 0, \alpha_t = \mathbf{1}(t)$	lift due to α_t (neglected)

Table 2. Geometrical characteristics of two aircraft.

Characteristic	Fighter	Transport
$S, \text{ m}^2$	27.9	511.0
$b, \text{ m}$	9.14	60.0
$\bar{c}, \text{ m}$	3.45	8.3
Λ	3.0	7.0
$S_p, \text{ m}^2$	4.55	142.0
$b_p, \text{ m}$	5.49	22.0
$\bar{c}_p, \text{ m}$	1.45	6.4
Λ_t	6.6	3.4
$L, \text{ m}$	4.59	30.0
$\ell, \text{ m}$	2.00	24.0
V_t	0.22	1.0
h	0.05	0.05

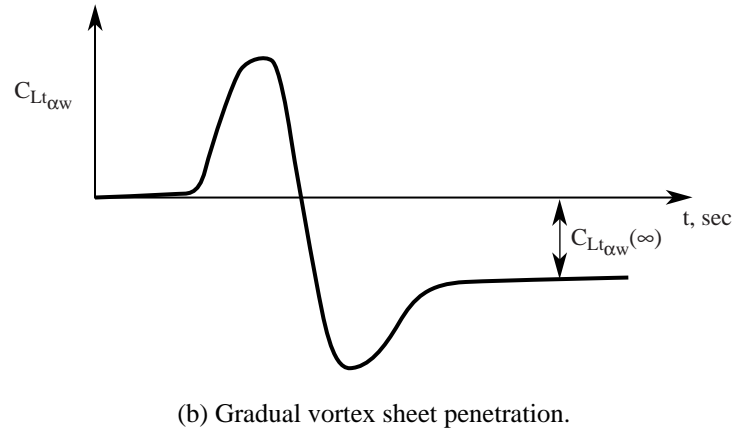
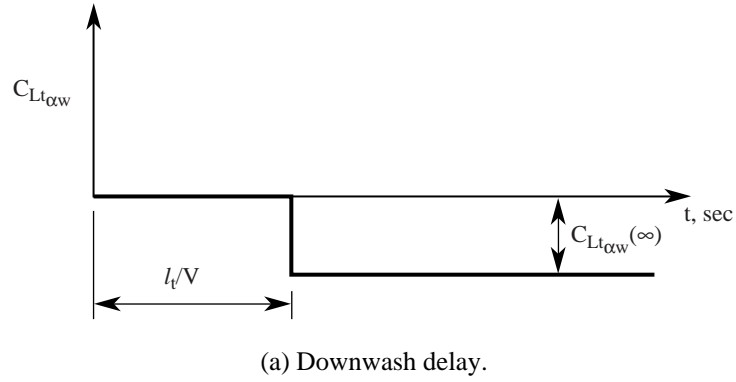


Figure 1. Qualitative time histories of tail lift caused by unit step in wing angle of attack.

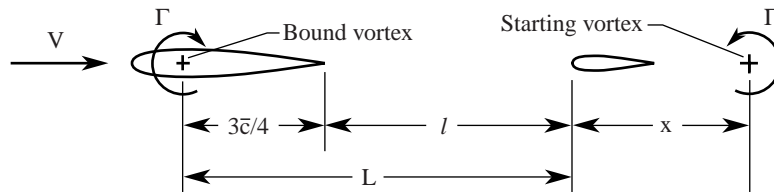


Figure 2. Location of bound and starting vortices.

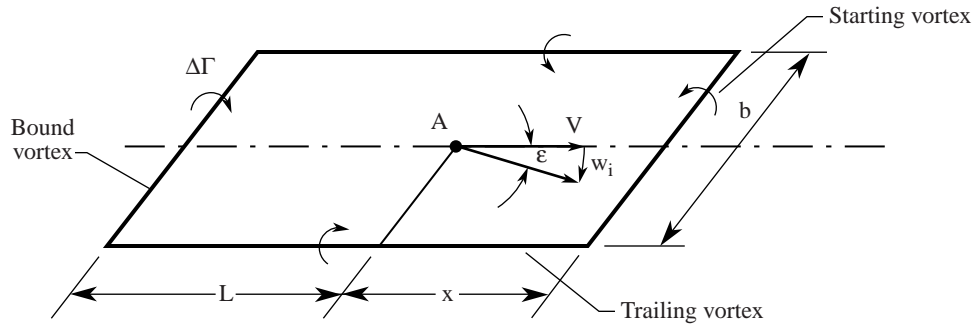


Figure 3. Vortex system used for computing downwash.

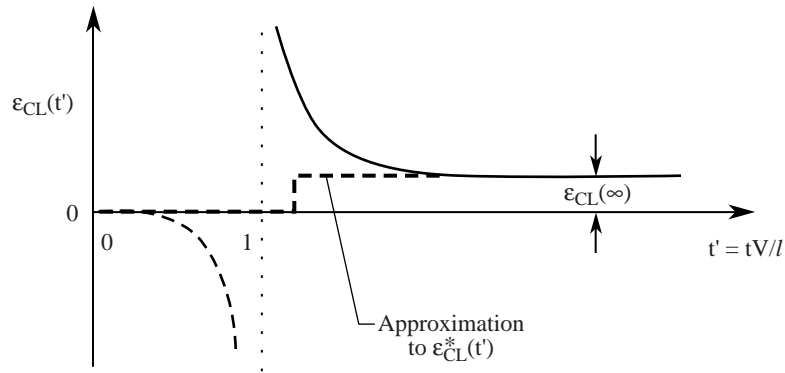


Figure 4. Sketched time histories of downwash indicial function and its approximation.

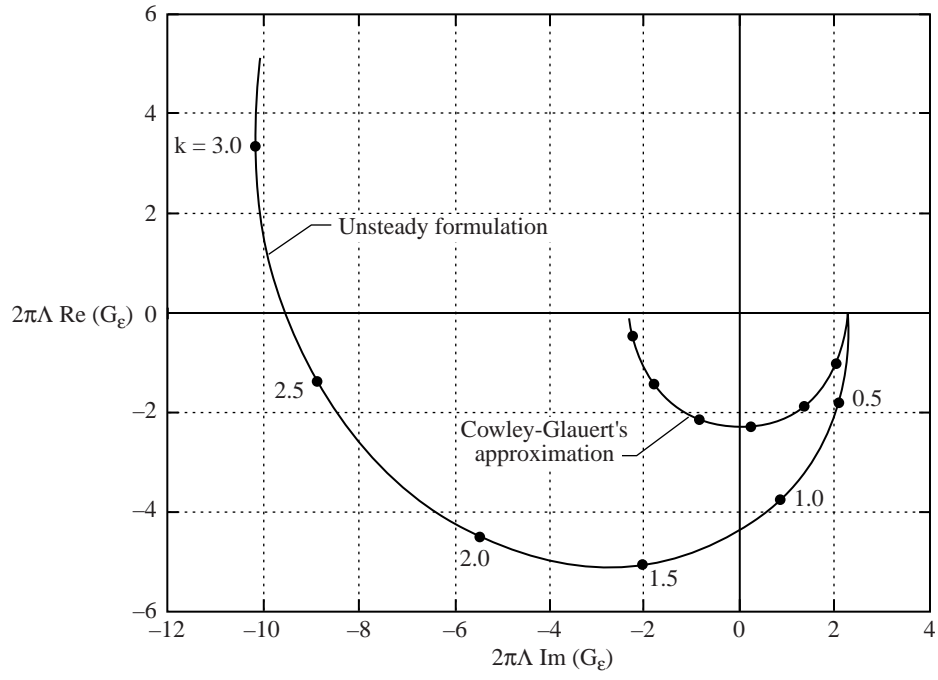


Figure 5. Frequency response curve relating downwash at the tail and lift on the wing. $\ell^1 = 1.0$

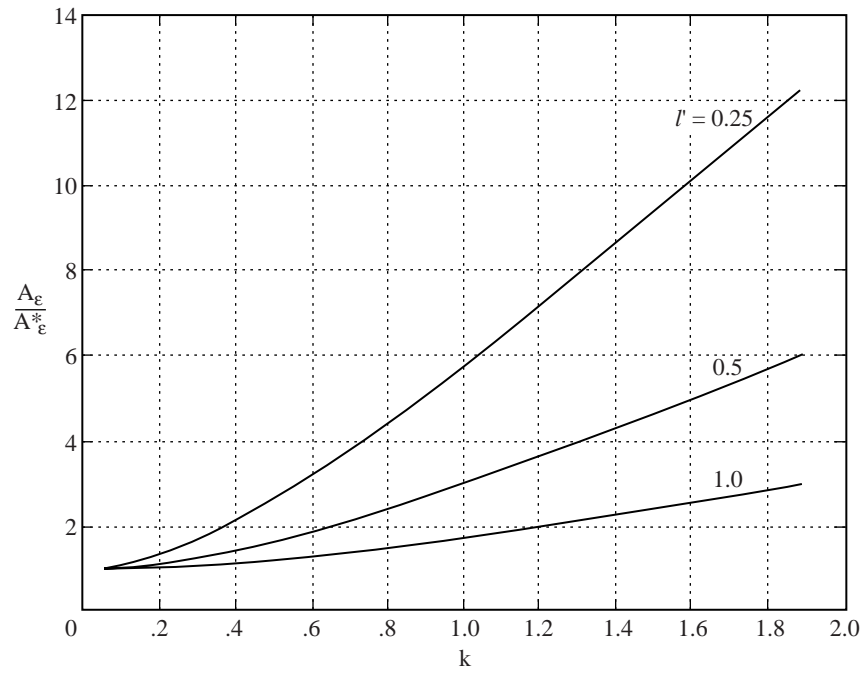


Figure 6. Amplitude ratio of harmonic downwash from unsteady and Cowley-Glauert's formulation.

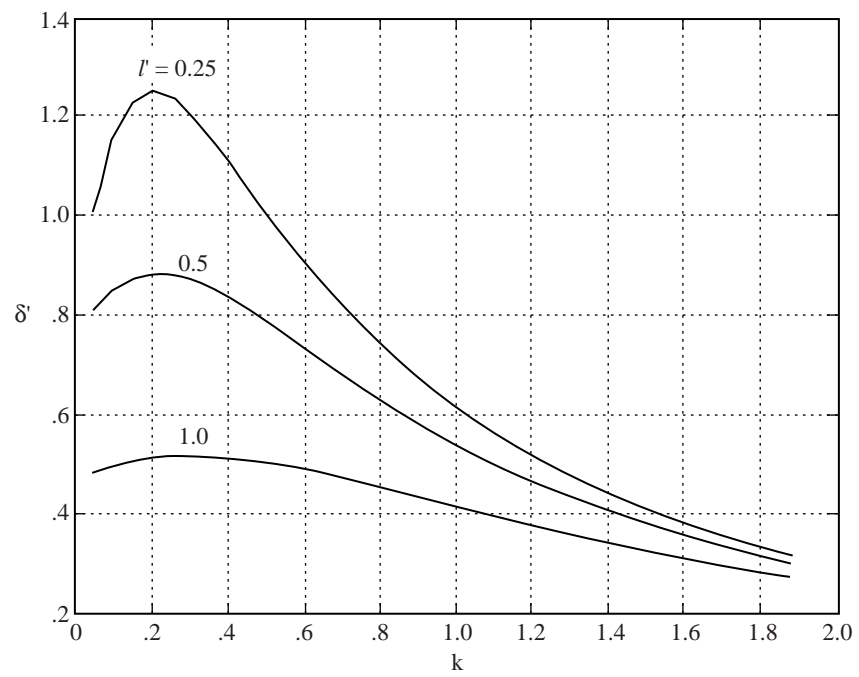


Figure 7. Difference in time delays of harmonic downwash from unsteady and Cowley-Glauert's formulation.

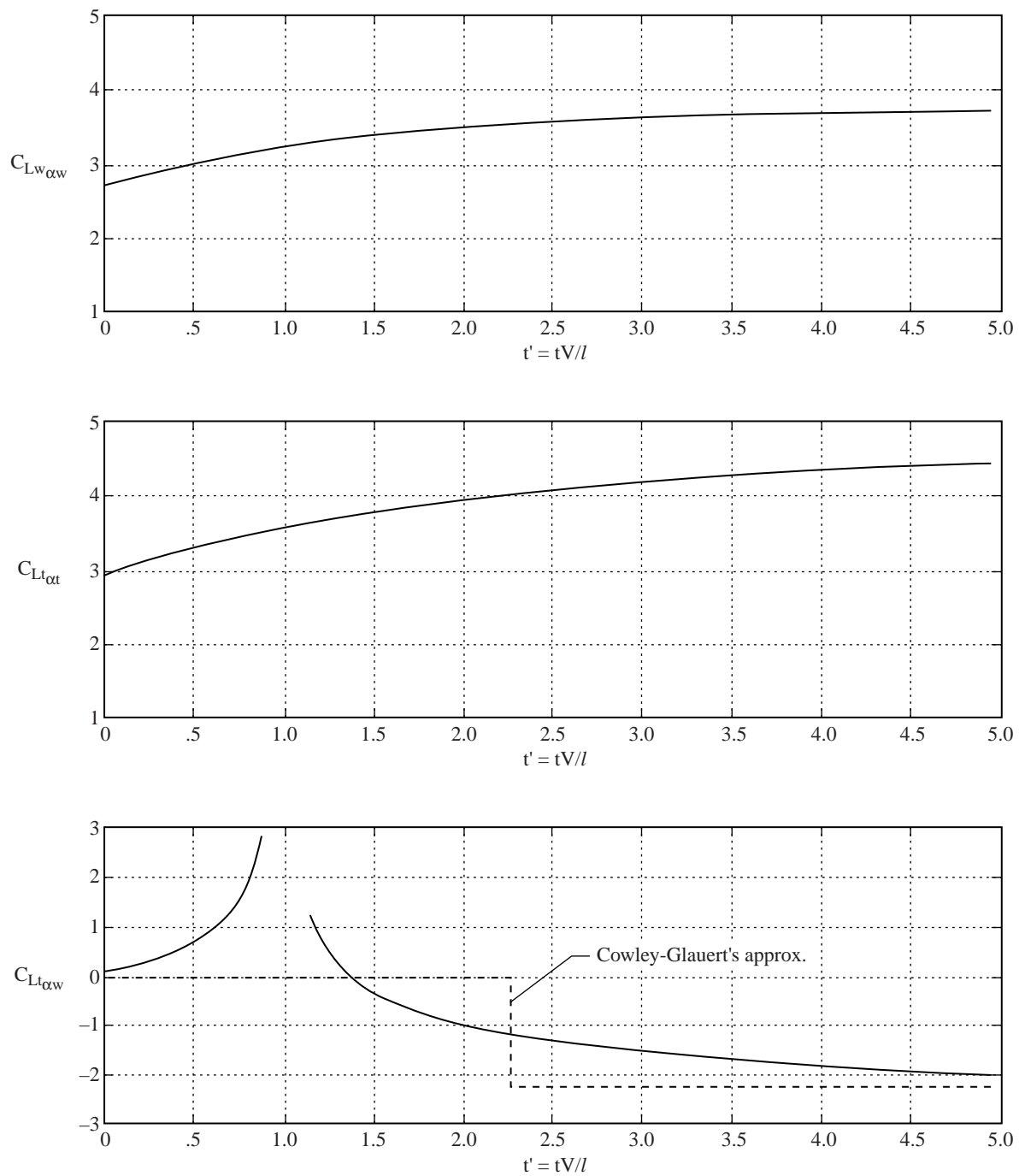


Figure 8. Indicial functions of wing and tail. Fighter aircraft.

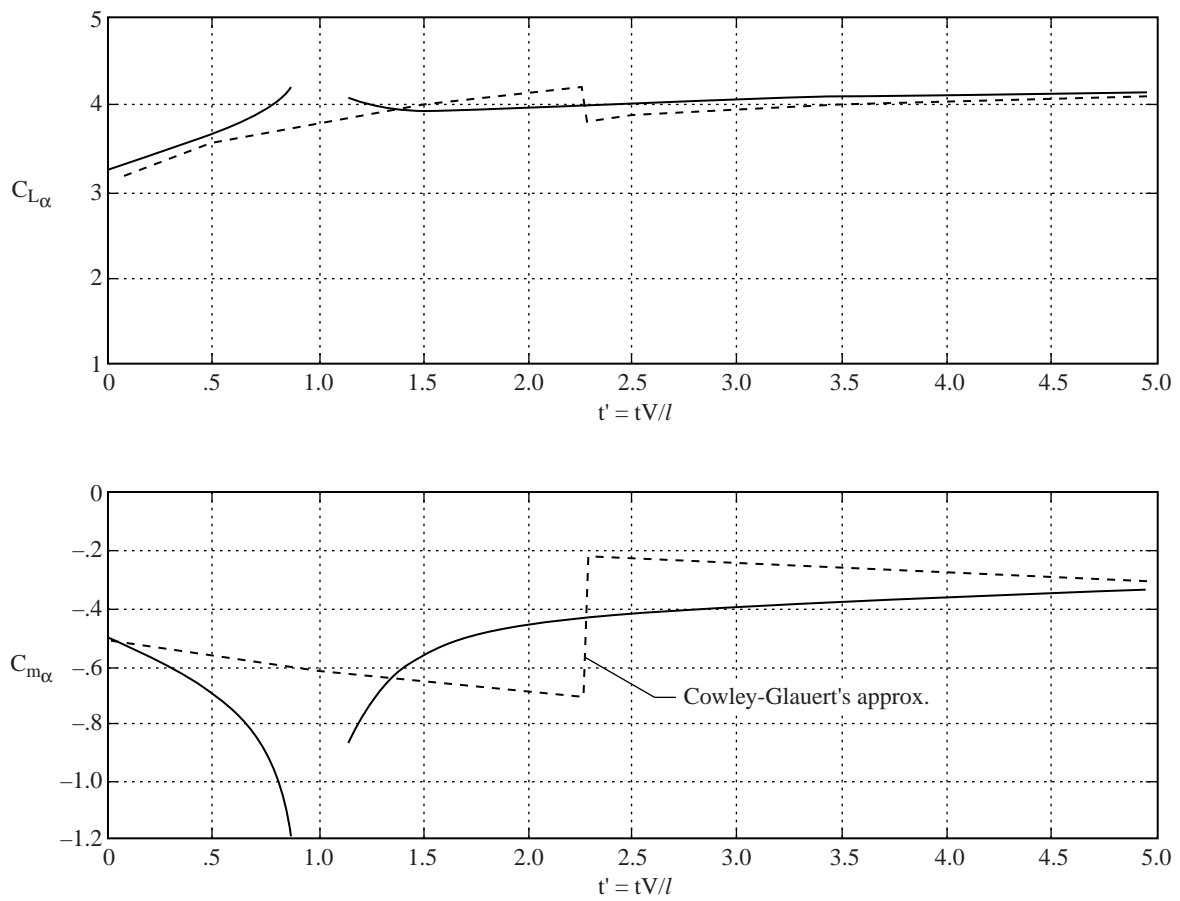


Figure 9. Indicial functions of wing-tail combination. Fighter aircraft.

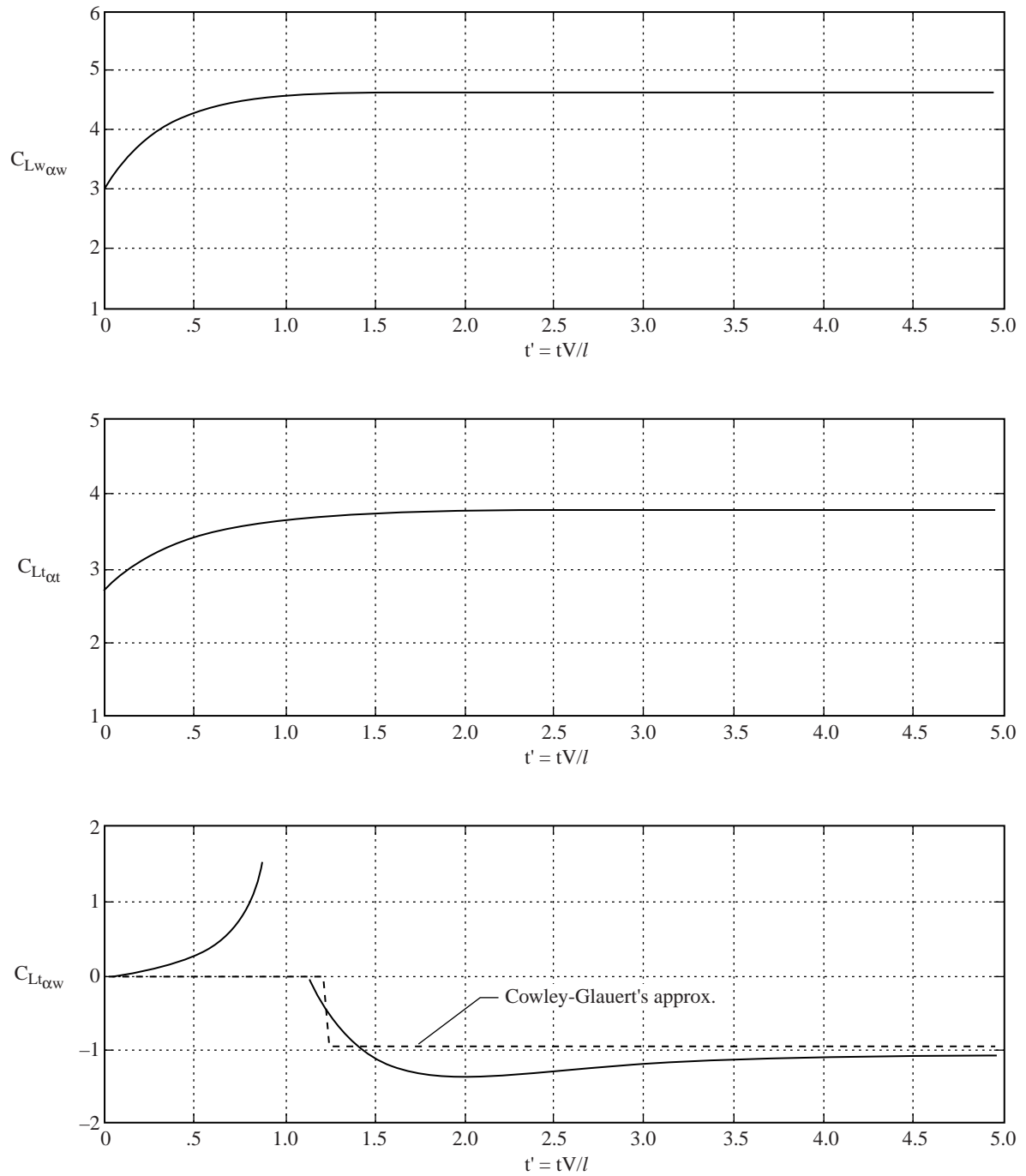


Figure 10. Indicial functions of wing and tail. Transport aircraft.

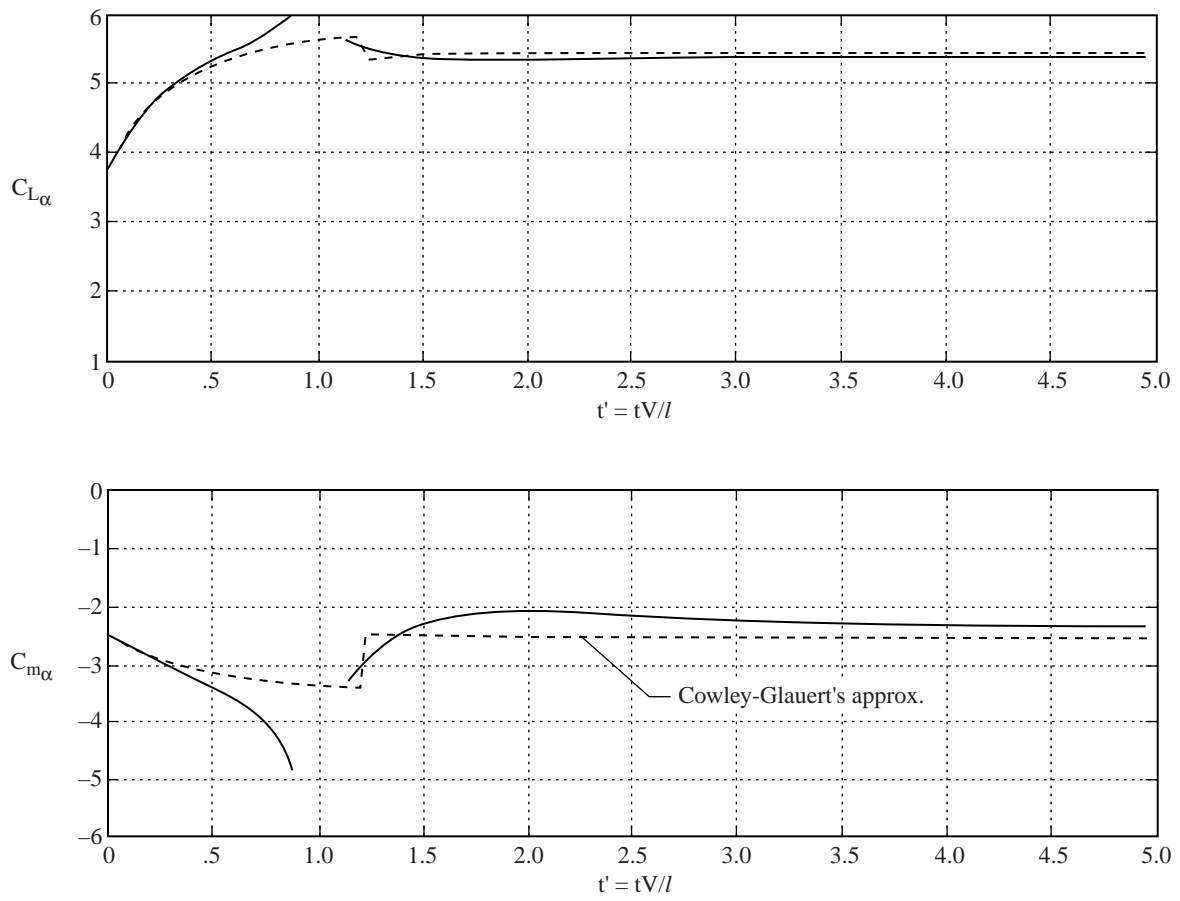


Figure 11. Indicial functions of wing-tail combination. Transport aircraft.

REPORT DOCUMENTATION PAGE			Form Approved OMB No. 07704-0188	
Public reporting burden for this collection of information is estimated to average 1 hour per response, including the time for reviewing instructions, searching existing data sources, gathering and maintaining the data needed, and completing and reviewing the collection of information. Send comments regarding this burden estimate or any other aspect of this collection of information, including suggestions for reducing this burden, to Washington Headquarters Services, Directorate for Information Operations and Reports, 1215 Jefferson Davis Highway, Suite 1204, Arlington, VA 22202-4302, and to the Office of Management and Budget, Paperwork Reduction Project (0704-0188), Washington, DC 20503.				
1. AGENCY USE ONLY (Leave blank)		2. REPORT DATE September 1999		3. REPORT TYPE AND DATES COVERED Contractor Report
4. TITLE AND SUBTITLE Modeling of Longitudinal Unsteady Aerodynamics of a Wing-Tail Combination			5. FUNDING NUMBERS NCC1-29 522-33-11-05	
6. AUTHOR(S) Vladislav Klein				
7. PERFORMING ORGANIZATION NAME(S) AND ADDRESS(ES) The George Washington University Joint Institute for Advancement of Flight Sciences (JIAFS) Langley Research Center Hampton, VA 23681-2199			8. PERFORMING ORGANIZATION REPORT NUMBER	
9. SPONSORING/MONITORING AGENCY NAME(S) AND ADDRESS(ES) National Aeronautics and Space Administration Langley Research Center Hampton, VA 23681-2199			10. SPONSORING/MONITORING AGENCY REPORT NUMBER NASA/CR-1999-209547	
11. SUPPLEMENTARY NOTES Langley Technical Monitor: James G. Batterson				
12a. DISTRIBUTION/AVAILABILITY STATEMENT Unclassified-Unlimited Subject Category 08 Availability: NASA CASI (301) 621-0390			12b. DISTRIBUTION CODE	
13. ABSTRACT (Maximum 200 words) Aerodynamic equations for the longitudinal motion of an aircraft with a horizontal tail were developed. In this development emphasis was given on obtaining model structure suitable for model identification from experimental data. The resulting aerodynamic models included unsteady effects in the form of linear indicial functions. These functions represented responses in the lift on the wing and tail alone, and interference between those two lifting surfaces. The effect of the wing on the tail was formulated for two different expressions concerning the downwash angle at the tail. The first expression used the Cowley-Glauert approximation known as "lag-in-downwash," the second took into account growth of the wing circulation and delay in the development of the lift on the tail. Both approaches were demonstrated in two examples using the geometry of a fighter aircraft and a large transport. It was shown that the differences in the two downwash formulations would increase for an aircraft with long tail arm performing low-speed, rapid maneuvers.				
14. SUBJECT TERMS aircraft longitudinal motion, unsteady aerodynamics, indicial functions			15. NUMBER OF PAGES 29	
			16. PRICE CODE A03	
17. SECURITY CLASSIFICATION OF REPORT Unclassified	18. SECURITY CLASSIFICATION OF THIS PAGE Unclassified	19. SECURITY CLASSIFICATION OF ABSTRACT Unclassified	20. LIMITATION OF ABSTRACT UL	